THE JOURNAL OF PHYSICAL CHEMISTRY A

Article

pubs.acs.org/JPCA

Hydrogen Bond Geometries and Proton Tautomerism of Homoconjugated Anions of Carboxylic Acids Studied via H/D Isotope Effects on ^{13}C NMR Chemical Shifts

Jing Guo,[†] Peter M. Tolstoy,*[,‡] Benjamin Koeppe,[∥] Nikolai S. Golubev,[§] Gleb S. Denisov,[§] Sergei N. Smirnov,[‡] and Hans-Heinrich Limbach[†]

[†]Institut für Chemie und Biochemie, Freie Universität Berlin, Takustrasse 3, D-14195 Berlin, Germany

[‡]Department of Chemistry, St. Petersburg State University, Universitetsky Pr. 26, 198504, St. Petersburg, Russia

[§]Department of Physics, St. Petersburg State University, Uljanovskaja 1, 198504, St. Petersburg, Russia

[∥]Max Born Institut für Nichtlineare Optik und Kurzzeitspektroskopie, Max Born Strasse 2A, D-12489 Berlin, Germany

ABSTRACT: Ten formally symmetric anionic OHO hydrogen bonded complexes, modeling Asp/Glu amino acid side chain interactions in nonaqueous environment (CDF_3/CDF_2Cl solution, 200−110 K) have been studied by ^{1}H, ^{2}H, and ^{13}C NMR spectroscopy, i.e. intermolecularly H-bonded homoconjugated anions of acetic, chloroacetic, dichloroacetic, trifluoroacetic, trimethylacetic, and isobutyric acids, and intramolecularly H-bonded hydrogen succinate, hydrogen *rac*-dimethylsuccinate, hydrogen maleate, and hydrogen phthalate. In particular, primary H/D isotope effects on the hydrogen bond proton signals as well as secondary H/D isotope effects on the ^{13}C signals of the carboxylic groups are reported and analyzed. We demonstrate that in most of the studied systems there is a degenerate proton tautomerism between O−H···O$^-$ and O$^-$···H−O structures which is fast in the NMR time scale. The stronger is the proton donating ability of the acid, the shorter and more symmetric are the H-bonds in each tautomer of the homoconjugate. For the maleate and phthalate anions exhibiting intramolecular hydrogen bonds, evidence for symmetric single well potentials is obtained. We propose a correlation between H/D isotope effects on carboxylic carbon chemical shifts and the proton transfer coordinate, $q_1 = {}^1/_2(r_{OH} - r_{HO})$, which allows us to estimate the desired OHO hydrogen bond geometries from the observed ^{13}C NMR parameters, taking into account the degenerate proton tautomerism.

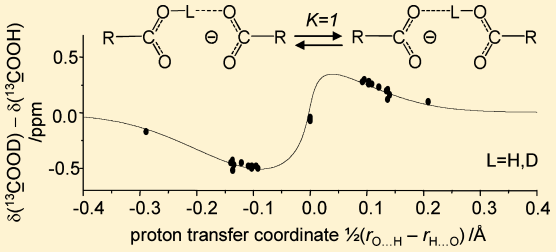

INTRODUCTION

Tertiary structures of proteins, which are essential for their function,[1−3] are often held together by H-bonds. One example of such hydrogen bonding is the interaction between carboxylic groups of aspartic (Asp) or glutamic (Glu) acid side chains. The steric proximity and closely matching proton accepting/donating abilities of Asp and/or Glu side chains often create conditions in which a short H-bond is likely to form, with a shared proton highly delocalized over acceptor and donor positions.[4−7] Short (O···O < 2.6 Å) hydrogen bonds between Asp and/or Glu side chains are found in 9% of proteins with such contacts,[8] for example in HIV-1 Protease[2,9] or rhamnogalacturonan acetylesterase (RGAE).[8] The bridging proton positions between carboxylates, i.e. the O···H and H···O distances, are often important for the stability and function of the biomolecule. However, these distances cannot be easily predicted, because in the hydrophobic areas of a biomolecule, steric constraints, local electric fields, and/or cooperativity effects in systems with several coupled H-bonds affect the H-bond geometry.

While in the solid state the hydrogen bond geometry can be obtained by X-ray diffraction or neutron scattering,[10−12] for biomolecules in solution one has to rely on spectroscopic techniques and NMR as the most widely used methods. Whereas for NHN and OHN hydrogen bonds ^{15}N substitution provides interesting NMR hydrogen bond correlations[13−16] which have been applied to biomolecules,[17,18] it is much more difficult to obtain information about the geometries of OHO by NMR because of the absence of a nucleus with spin $^1/_2$. Here, only the ^{1}H chemical shift of the bridging proton, $\delta(^1H)$, has been correlated in the past with the O···O, O···H, and H···O distances for OHO type hydrogen bonds.[14,19−23] However, for a biomolecule in aqueous solution, the observation of bridging proton signals is often hindered by the proton exchange with solvent molecules.[24] For a pair of interacting carboxylates, the nucleus with spin $^1/_2$ located most closely to the hydrogen bond is the carboxylic carbon (^{13}C). This nucleus does not exchange with the solvent, though the absolute value of the chemical shift, $\delta(^{13}\underline{C}OOH)$, is strongly influenced by the nature of the substituents and the local environment.[25−27] This is

Special Issue: A: Jorn Manz Festschrift

Received: May 22, 2012
Revised: June 27, 2012
Published: June 27, 2012

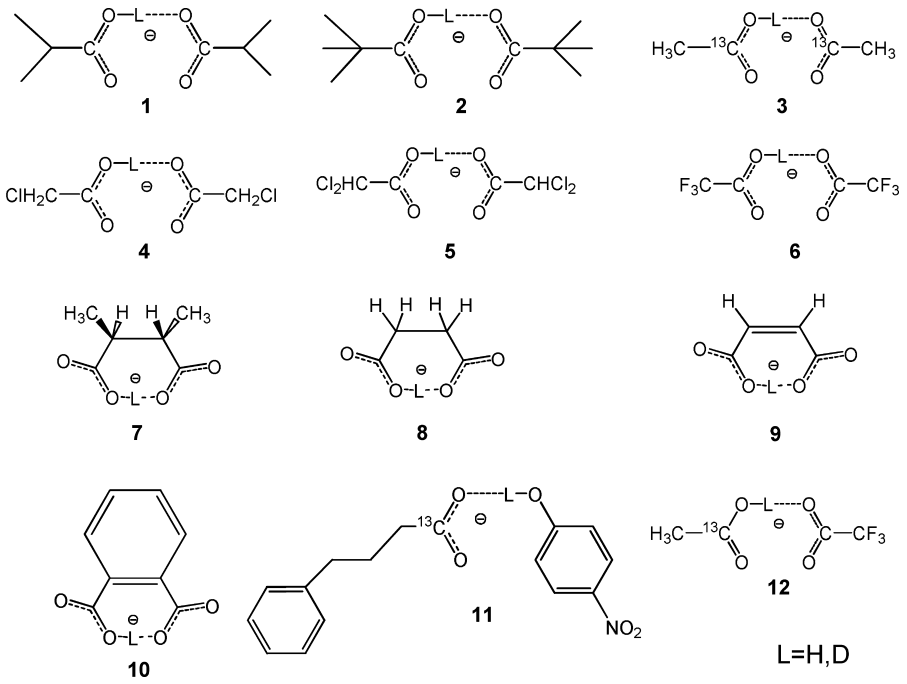

Figure 1. Schematic structures of inter- and intramolecularly hydrogen bonded complexes **1**−**12** studied in this work. Tetraethylammonium (for **1**, **2**, **4**−**8**, **10**−**12**) and tetrabutylammonium (for **3** and **9**) used as counter-cations are not shown.

disadvantageous for using $\delta(^{13}\underline{C}OOH)$ as a reporter of the H-bond properties. However, a more useful NMR parameter is the H/D isotope effect on the chemical shift, $^{2}\Delta C(D) \equiv \delta(^{13}\underline{C}OOD) - \delta(^{13}\underline{C}OOH)$. This differential quantity has the substituent effects and the local environment effects canceled, so that the resulting value reflects mostly the change of the H-bond properties upon deuteration. For example, H/D isotope effects on ^{13}C chemical shifts were previously used for structure analysis of the active site of the HIV-1 Pr/pepstatin complex, assuming simply that the presence/absence of the measurable isotope effect on the chemical shift is indicative of the protonated/deprotonated state of a carboxylic group.[2,28] A more systematic study of $^{2}\Delta C(D)$ for OHO hydrogen bonds was attempted previously[29] using model systems, although only a semiquantitative interpretation of isotope effects was given. It was pointed out that the absence of the measurable H/D isotope effect is consistent both with a SSHB (short strong hydrogen bond) and a very weak OHO hydrogen bond.[29] Recently, a quantitative analysis has been performed for intermolecular OHN bonds in carboxylic acid complexes with pyridines.[30] We note that, apart from the nearest carbon, the NMR parameters of the nearest CH proton might have diagnostic value for determining the geometry of OHO hydrogen bonds. For example, the chemical shift of the ortho-proton of 2-chloro-4-nitrophenol and the secondary isotope effect on it after bridge proton H/D substitution follow the proton transfer pathway in a series of heteroconjugate complexes.[31] However, CH lines are often broadened due to the hydrogen bond exchange processes, and it is not easy to resolve the H/D effects, which are usually less than 0.05 ppm.

In this paper we focus on short OHO bonds in carboxylic acid−carboxylate model systems, mimicking a possible interaction between Asp and/or Glu side chains. Our main goal is 2-fold. First, we want to find out qualitatively the shapes of proton stretching potentials and estimate the hydrogen bond geometries in a series of structurally similar homoconjugated anionic complexes. Second, pursuing our long-term goal of establishing correlations between H-bond geometry and experimental NMR parameters, we want to construct an empirical correlation between $^{2}\Delta C(D)$, and the bridging proton position inside the OHO hydrogen bond.

Before we present the complexes selected for this study, we would like to point out that carboxylic acid−cabroxylate systems often show proton tautomerism, i.e. exchange between two equilibrium proton positions, O−H···O$^-$ and O$^-$···H−O, which might be nonequivalent.[32] The corresponding proton transfer rates vary in a broad range, depending on the system studied, often being 10^6−10^9 Hz for various complexes with medium-strong H-bonds.[33−35] Such proton tautomerism is fast on the NMR time scale, and each observed NMR parameter δ is then a weighted average

$$\delta_{obs} = x_\alpha \delta_\alpha + x_\beta \delta_\beta \quad (1)$$

where x_α and x_β are mole fractions of tautomers, $x_\alpha + x_\beta = 1$, and δ_α and δ_β are intrinsic NMR parameters. In general, x_α, x_β, δ_α, and δ_β cannot be obtained from a single value of δ_{obs}, and thus a proper correlation between NMR observables and hydrogen bond geometry is hard to establish. Moreover, each additional measured NMR parameter would also be averaged over two unknown intrinsic values, and as a result, the number of equations, such as eq 1, is always insufficient to solve for unknowns.

In order to reduce the number of unknowns, for this work we have chosen formally symmetric systems 1−10, whose structures are schematically shown in Figure 1. Complexes were dissolved in a mixture of liquefied gases, CDF_3/CDF_2Cl, and studied by ^{1}H, ^{2}H, and ^{13}C NMR spectroscopy in the temperature range 110−200 K. NMR spectra of complexes **3**, **4**, **7**, **8**, and **9** have been reported previously;[29,36,37] here we add these complexes to the set for the sake of completeness. In anions **1**−**10**, an OHO hydrogen bond links two chemically equivalent fragments either inter- (**1**−**6**) or intramolecularly

dx.doi.org/10.1021/jp304943h | J. Phys. Chem. A 2012, 116, 11180−11188

(**7**−**10**). The symmetry ensures that in the case where proton tautomerism is present, the statistical weights of the tautomers would be the same, $x_\alpha = x_\beta = 0.5$ (see Figure 2). Fortunately,

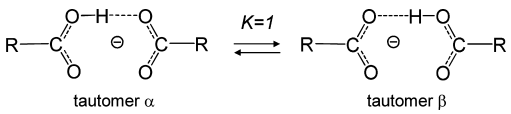

Figure 2. Schematic representation of proton tautomerism in homoconjugated carboxylic acid−carboxylate complexes.

proton tautomerism between two chemically equivalent positions would also lead to $\delta H_{obs} = \delta H_\alpha = \delta H_\beta$, which would allow us to use the δH_{obs} value to estimate the hydrogen bond geometry.[22] In contrast, observed values of $^2\Delta C(D)$ are still subject to averaging over two unknown intrinsic values. Thus, in order to reach the main goal in this work, we would have to find a way to extract intrinsic values $^2\Delta C(D)_\alpha$ and $^2\Delta C(D)_\beta$ from the average ones. For this reason, we have included into our study two heteroconjugated anions: complex of 4-phenylbutyric acid with *p*-nitrophenolate (**11**) and complex of acetic acid with trifluoroacetate (**12**) (tetraethylammonium as countercation in both cases). The usefulness of **11** and **12** will be demonstrated in the Discussion.

EXPERIMENTAL PART

Chemicals. Commercially available 1-^{13}C-labeled acetic acid ($CH_3{}^{13}COOH$, 99% ^{13}C), deuterium oxide ($D_2O \geq 99.90\%$), and CH_3OD (99% D) were purchased from Eurisotop GmbH; chloroacetic acid/anhydride, dichloroacetic acid/anhydride, trifluoroacetic acid, phthalic acid, as well as a 1.5 M methanol solution of tetraethylammonium (TEA) hydroxide were purchased from Aldrich and used without further purification.

Sample Preparation for Complexes 3, 4, 7, 8, and 9. The spectra of these complexes shown in this work are adapted from our previously published works. The sample preparation is described in ref 29 for **3** and **4**, in ref 36 for **7** and **8**, and in ref 37 for **9**.

Sample Preparation for Complexes 1, 2, 5, and 6. First, TEA salts were prepared by mixing the corresponding acids and TEA hydroxide with a 1:1 ratio. Methanol and water were removed on a rotary evaporator by repeatedly adding and pumping away CH_2Cl_2. The resulting solid substance was redissolved in CD_2Cl_2, and a small amount of the solution was transferred into a NMR sample tube and dried overnight under vacuum. Subsequently, 0.6 equiv of a partially deuterated acid, freshly prepared by mixing the corresponding anhydride and D_2O, was added to the sample tube.

Sample Preparation for Complex 10. TEA hydrogen phthalate was prepared by mixing the CH_2Cl_2 solution of phthalic acid with 1 equiv of TEA hydroxide solution; then distilled CH_2Cl_2 (2−3 mL) was repeatedly added to the reaction mixture and pumped out on a rotary evaporator to remove H_2O and CH_3OH, leaving solid product. TEA hydrogen phthalate was deuterated at a mobile proton site by dissolving it twice in CH_3OD and removing the solvent on a rotary evaporator. The necessary amount was weighed in the NMR sample tube. The final deuteration step was performed by adding CH_3OD directly into the sample tube and removing the solvent under high vacuum for ca. 12 h.

Sample Preparation for Complex 11. Heteroconjugated anion **11** was prepared according to the procedure described in ref 60.

Sample Preparation for Complex 12. First, the TEA salt of trifluoroacetic acid was prepared in the same way as for **6**. After that the necessary amount was transferred to the NMR sample tube. 0.5 equiv of 1-^{13}C-labeled acetic acid deuterated at the mobile proton position as described in ref 29 was subsequently added to the NMR sample tube already containing TEA trifluoroacetate.

Freonic Solvent. The solvent, CDF_3/CDF_2Cl (freezing point below 100 K), prepared by the modified method described in ref 38 was added to the samples by vacuum transfer. The overall concentration of the complex in the sample, estimated by measuring the volume of the solution at low temperatures (around 120 K), was about 0.1 M.

NMR Measurements. Thick-walled sample NMR tubes equipped with PTFE valves (Wilmad, Buena) were used (except for complex **11**, for which a quartz medium-walled sample tube was used). NMR spectra were measured on a Bruker Avance-500 NMR spectrometer equipped with a low-temperature probe, which allowed us to perform experiments down to 100 K. ^{1}H NMR spectra were measured in the temperature range from 200 to 110 K. Chemical shifts were measured using CHF_2Cl as internal standard and converted to the conventional TMS scale. Combined NMR and UV measurements for complex **11** were performed using the experimental setup described in ref 60.

Hydrogen Bond Correlations. It has been shown by neutron diffraction that for OHO hydrogen bonds the interatomic distances r_{OH} and r_{HO} or their linear combinations

$$q_1 = {}^1\!/_2(r_{OH} - r_{HO})$$
$$q_2 = r_{OH} + r_{HO} \quad (2)$$

are interdependent.[39] q_2 describes the distance between two oxygen atoms along the hydrogen bond, and q_1 is a measure of hydrogen bond asymmetry. During the past decade, this interdependence was described by the valence bond order model, which was later on corrected to take into account quantum zero point vibrational effects.[13,22,40,41] It has been shown that the valence bond orders can be correlated with various NMR parameters.[29,30,42−46] The correlation equations were rather cumbersome and nonexplicit, so for simplicity, in ref 22 an empirical equation was proposed for the explicit dependence of bridging proton chemical shift $\delta(O\underline{H}O)$ on H-bond asymmetry parameter q_1, which was shown to be numerically equivalent to the results of the valence bond order model:

$$\delta(O\underline{H}O) = \delta^\circ_{OH} + \Delta_H \exp(-aq_1^2) \quad (3)$$

where $\delta^\circ_{OH} = 6$ ppm is the limiting chemical shift for the free monomeric carboxylic acid;[47] $\Delta_H = 15$ ppm leads to the maximum proton chemical shift of 21 ppm, corresponding to the strongest hydrogen bond,[29,48] and $a = 6.2$ Å^{-1} is an empirical fitting parameter.

RESULTS

Figure 3a shows the low-field parts of the low-temperature ^{1}H (solid line) and ^{2}H (dashed line) NMR spectra of the samples containing homoconjugated monoanions **1**−**10** dissolved in CDF_3/CDF_2Cl. The spectra of **9** have been adapted from ref

dx.doi.org/10.1021/jp304943h | J. Phys. Chem. A 2012, 116, 11180−11188

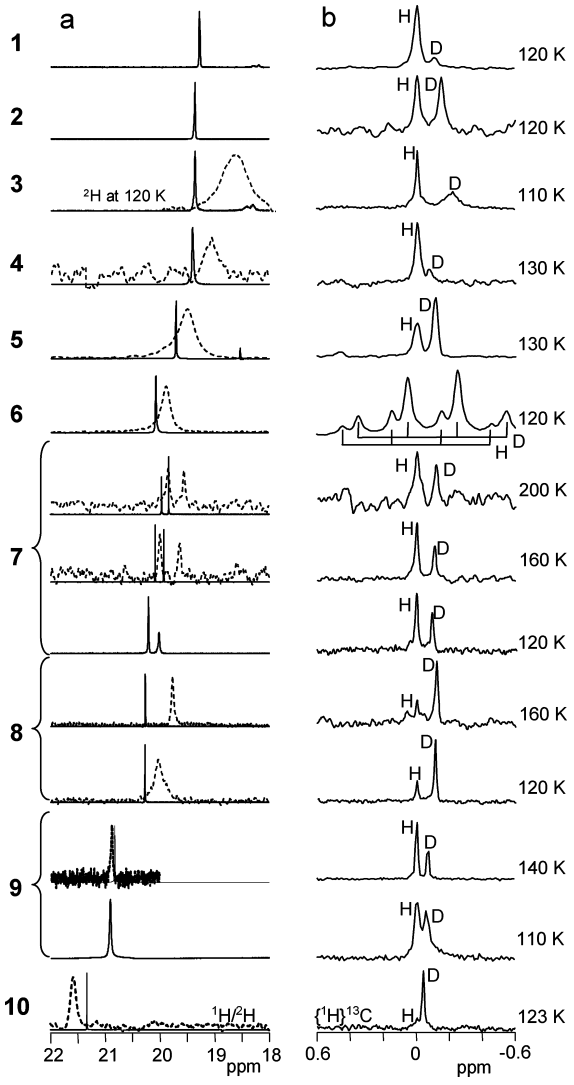

Figure 3. (a) Low-field parts of ^{1}H (solid lines) and ^{2}H (dashed lines) spectra of homoconjugated complexes **1**−**10** dissolved in CDF_3/CDF_2Cl at selected temperatures. In the case of complex **7**, two ^{1}H and ^{2}H NMR signals correspond to *meso*- and *rac*-isomers; the racemic form gives the lower field signals in both cases. (b) Parts of ^{13}C NMR spectra of homoconjugated complexes **1**−**10**; signals from the deuterated and nondeuterated forms are marked with "D" and "H", respectively. For clarity, the "H" signal was calibrated to 0 ppm. All the data are collected in Table 1. The spectra of **9** have been adapted from ref 29, as well as the ^{2}H and ^{13}C spectra of **3**. The spectra of **7** and **8** have been adapted from ref 36. The temperatures at which the spectra shown in parts a and b were measured are given near the curves.

29, as well as the ^{2}H and ^{13}C spectra of **3**. The spectra of **7** and **8** have been adapted from ref 36. Generally, singlets are observed for the bridging protons and deuterons, where the ^{2}H signals are broadened by quadrupole relaxation. The spectra of complex **7** exhibit two bridging proton signals. The one at lower field arises from the racemic form of dimethylsuccinic acid monoanion, while the one at higher field stems from the *meso*- form.[36] The *meso*- form has lower symmetry than the *rac*-form;[36] thus, it is not a formally symmetric homoconjugate and will not be considered in this work.

In Figure 3b the parts of corresponding ^{13}C NMR spectra are shown, displaying the signals of carboxylic carbons. The ^{13}C chemical shifts are scattered in a 17 ppm range; therefore, in order to simplify the following discussion, all ^{13}C NMR signals were referenced internally to those of the protonated forms of the monoanions, set to 0 ppm; the values referenced to tetramethylsilane are listed in Table 1. Signals from the deuterated and nondeuterated forms of a complex are marked with "D" and "H", respectively. The secondary H/D isotope effects on the carbon chemical shift, defined as $^2\Delta C(D) = \delta(^{13}\underline{C}OOD) - \delta(^{13}\underline{C}OOH)$, are negative for all complexes **1**−**10**. The relative intensities of $^{13}\underline{C}OOD$ and $^{13}\underline{C}OOH$ signals depend on the deuteration fraction of the sample, which was quite difficult to precisely control. The signals of the protonated and deuterated forms of complex **6** are split into quartets due to the $^2J_{CF}$ scalar coupling of ca. 37 Hz. All NMR parameters of complexes **1**−**10** are collected in Table 1.

In Figure 4 are depicted the NMR and UV−vis spectra of the hydrogen bonded complex of 4-phenylbutyric acid with *p*-nitrophenolate (**11**) as well as NMR spectra of the complex of acetic acid with trifluoroacetate anion (**12**). Although complexes **11** and **12** do not belong to the category of homoconjugated anions, they offer great help when processing the data of homoconjugates, as shown later in the Discussion. In the ^{1}H NMR spectra of **11** and **12**, we observe signals at about 17 ppm and 14 ppm, respectively, indicating medium−strong hydrogen bonds (Figure 4a). As the carboxylic groups of **11** and of **12** were labeled with ^{13}C (see Figure 1), only the signals of these groups are visible. The secondary H/D isotope effects on δ^{13}C for **11** and **12** have opposite signs: positive for **11** and negative for **12** (Figure 4b). In Figure 4c the UV−vis spectrum of **11** measured at 120 K using the newly established UVNMR technique[60] is shown. UVNMR allows simultaneous registration of NMR and UV−vis spectra of the same sample inside the magnet of an NMR spectrometer, which guarantees that all spectroscopic information is consistent and obtained under identical conditions. For **11**, the UV−vis spectrum has a single absorption maximum at ca. 350 nm. The interpretation of the band will be given in the Discussion. The NMR data of complexes **11** and **12** are included in Table 1.

DISCUSSION

We have measured bridging proton chemical shifts, δH, and H/D isotope effects on carboxylic carbon chemical shifts, $^2\Delta C(D)$, for ten homoconjugated anions (**1**−**10**) and two heteroconjugated anions (**11**, **12**) dissolved in CDF_3/CDF_2Cl at 110−200 K. Our goal is to establish a link between the values of $^2\Delta C(D)$ and the bridging proton position inside the H-bond. To demonstrate how we have achieved this goal, we have structured the Discussion as follows. First, we qualitatively discuss the shape of the potential energy surfaces along the proton transfer coordinates for the complexes studied, which allows us to check for the possibility of proton tautomerism in each complex. Second, we estimate the O···H and H···O distances using experimental values of δH and previously established hydrogen bond correlations. Finally, we construct a new correlation between bridging proton positions and the values of $^2\Delta C(D)$. Based on this curve, in conclusion we propose an experimental criterion which allows one to distinguish between carboxylic acid−carboxylate H-bonded complexes with proton tautomerism (double-well potential) and without tautomerism (single-well potential). The proposed criterion is valid for both symmetric and asymmetric potentials.

Single vs Double Well Potentials. The homoconjugated anionic complexes **1**−**8** give rather low-field ^{1}H chemical shifts between 19.3 and 20.3 ppm, which are characteristic for short

dx.doi.org/10.1021/jp304943h | J. Phys. Chem. A 2012, 116, 11180−11188

Table 1. Experimental NMR Parameters, Estimated Hydrogen Bond Geometry, and Estimated Intrinsic ^{13}C NMR Parameters of Complexes 1−12[a]

substance	no.	T/K	δH/ ppm	δD/ ppm	δ(^{13}C̲OOH)/ ppm	δ(^{13}C̲OOD)/ ppm	$^{2}\Delta$C(D) /ppm	q_2/Å	$q_{1\alpha}$/Å	$q_{1\beta}$/Å	$\Delta\delta^{13}C_\alpha$/ ppm	$\Delta\delta^{13}C_\beta$/ ppm
hydrogen bis-isobutyrate	**1**	120	19.28		185.78	185.64	−0.14	2.453	−0.140	0.140	−0.45	+0.16
hydrogen bis-trimethylacetate	**2**	120	19.36		186.73	186.62	−0.11	2.451	−0.137	0.137	−0.43	+0.21
hydrogen bis-acetate	**3**	110	19.37	18.63	180.19	179.99	−0.20	2.451	−0.136	0.136	−0.52	+0.12
hydrogen bis-chloroacetate	**4**	130	19.41	19.06	173.45	173.32	−0.13	2.450	−0.134	0.134	−0.47	+0.20
hydrogen bis-dichloroacetate	**5**	130	19.71	19.51	170.07	169.96	−0.11	2.443	−0.120	0.120	−0.45	+0.23
hydrogen bis-trifluoroacetate	**6**	120	20.07	19.90	162.81	162.71	−0.10	2.435	−0.102	0.102	−0.48	+0.28
hydrogen *rac*-dimethyl succinate	**7**	200	19.97	19.86	182.66	182.55	−0.11	2.437	−0.107	0.107	−0.48	+0.26
		160	20.08	20.01	182.90	182.80	−0.10	2.434	−0.101	0.101	−0.48	+0.26
		120	20.21		183.09	183.00	−0.09	2.432	−0.093	0.093	−0.48	+0.30
hydrogen succinate	**8**	160	20.07	19.78	180.51	180.39	−0.12	2.435	−0.102	0.102	−0.50	+0.26
		120	20.27	20.06	180.74	180.63	−0.11	2.430	−0.090	0.090	−0.50	+0.28
hydrogen maleate	**9**	140	20.84	20.89	171.05	170.98	−0.07	2.415[b]	0[b]	0[b]		
		110	20.92		171.05	171.00	−0.05	2.415[b]	0[b]	0[b]		
hydrogen phthalate	**10**	123	21.33	21.58	172.27	172.23	−0.04	2.415[b]	0[b]	0[b]		
4-phenylbutyric acid/*p*-nitrophenolate	**11**	125	17.32		182.34	182.44	0.10	2.507		+0.217		+0.10
acetic acid/trifluoroacetate	**12**	120	14.57		177.22	177.05	−0.17	2.601	−0.301		−0.17	

[a]Experimental parameters: chemical shifts of bridging proton δH, bridging deuteron δD, and carboxylic carbons δ(^{13}C̲OOH) and δ(^{13}C̲OOD), as well as the secondary isotope effect $^{2}\Delta C(D) = \delta(^{13}\underline{C}OOD) - \delta(^{13}\underline{C}OOH)$. Carbon chemical shifts refer to the carboxylic carbon in 4-phenylbutyrate for **11** and in acetate for **12**. Estimated parameters: overall hydrogen bond length $q_2 = r_{OH} + r_{HO}$, its asymmetry $q_1 = {}^1/_2(r_{OH} - r_{HO})$, and predicted intrinsic values of $\Delta\delta^{13}C$ for complexes with degenerate proton tautomerism. [b]For complexes with a central-symmetric hydrogen bond, the geometry is estimated by setting q_1 to 0 and q_2 to its minimum value.

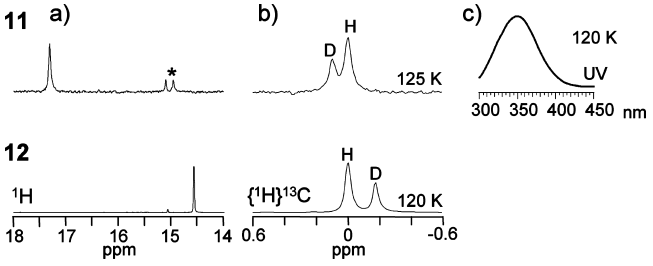

Figure 4. (a) Low-field part of ^1H spectra of heteroconjugated complexes **11** and **12** in CDF_3/CDF_2Cl. In **11**, signals marked with "*" are from the dihydrogen tricarboxylate complex, not discussed in this work. (b) Parts of ^{13}C NMR spectra of complexes **11** and **12**; signals from the protonated and deuterated forms are marked with "H" and "D", respectively. The "H" signal was calibrated to 0 ppm. Experimental data are collected in Table 1. (c) UV spectrum of **11**; the single band proves the presence of only one tautomer; see text for more detail. The temperatures at which the spectra shown in parts a and b were measured are given near the curves.

hydrogen bonds. Negative primary isotope effects, $\delta D - \delta H < 0$, indicate that the most probable bridging proton position for these complexes is not located in the hydrogen bond center.[29,49] Taking into account the formal symmetry of the complexes, this suggests a symmetric double-well potential along the proton transfer coordinate. Note, however, that in our case the complexes are surrounded by solvent cages whose structures influence the hydrogen bond geometries,[50,51] and the current disorder of the polar solvent molecules may break the hydrogen bond symmetries.[52,53] This means that for a fixed structure of a given solvent cage the "diabatic" proton stretching potential for **1**−**8** is likely to be an asymmetric single-well, as schematically shown by the horizontal dotted lines in Figure 5a. The "adiabatic" proton transfer coordinate which gives the symmetric double-well potential includes the reorientation of the solvent molecules (dashed curve in Figure 5a). In other words, by the term "proton transfer coordinate" we mean a collective mode which includes solvent coordinates and for which the bridging proton position is adjusted to the instantaneous solvent cage configuration. In liquid solution, different solvent configurations may be present which interconvert fast on the NMR but slowly in the UV−vis time scales.[54] Homoconjugates **9** and **10** exhibit between 110 and 120 K the largest proton chemical shifts of 20.8 and 21.3 ppm and the positive primary H/D isotope effects of +0.05 and +0.25 ppm. These values are larger than those reported previously,[55] indicating slightly stronger hydrogen bonds. This effect might arise from the polar solvent ordering at low temperatures which symmetrizes strong hydrogen bonds.[14,36] The secondary H/D isotope effects on the carbon chemical shifts are very small. These results suggest symmetric single-well potential with the single most probable proton position in the center of the H-bond, as illustrated in Figure 5b.[37,56] We note a recent discussion of the symmetries of strong hydrogen bonds. Perrin et al. have measured ^{18}O isotope effects on ^{13}C chemical shifts of maleate, phthalate, and derivatives,[53,57] which have been interpreted in terms of an equilibrium between nonsymmetric tautomers. Singleton et al. have reinterpreted these findings in terms of isotope-induced desymmetrization of symmetrical potential energy surfaces.[58] Some of us have proposed broad distributions of hydrogen bond geometries, which may exhibit either two or only one maximum.[54] That would imply that a true symmetric hydrogen bond might be in fast equilibrium with hydrogen bonds which are slightly perturbed by the environment.

dx.doi.org/10.1021/jp304943h | J. Phys. Chem. A 2012, 116, 11180−11188

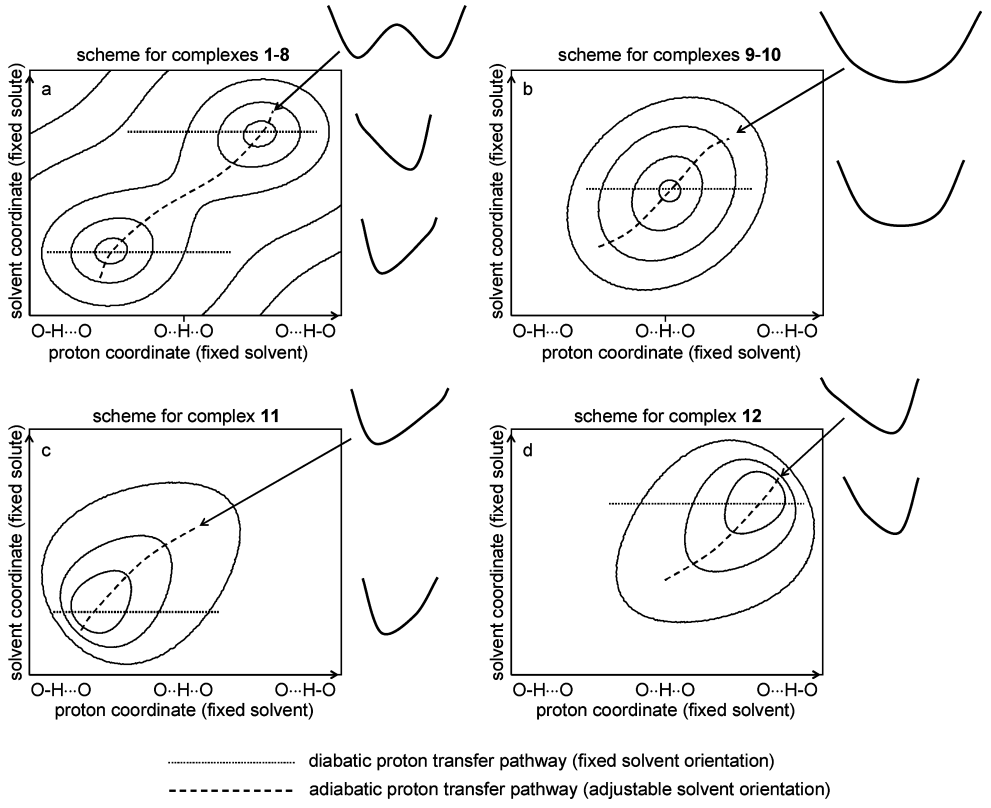

Figure 5. Schematic representation of the potential energy surface of the proton transfer for complexes **1**−**12**. For the sake of discussion, the surface is plotted using the "gas phase" proton transfer coordinate (fixed solvent) and the solvent coordinate (fixes solute). (a) Double-well potential for complexes **1**−**8**. (b) Center-symmetric potential for complexes **9** and **10**. (c and d) Asymmetric single-well potentials for complexes **11** and **12.** Shown surfaces do not correspond to any calculation and serve as a guide for the discussion.

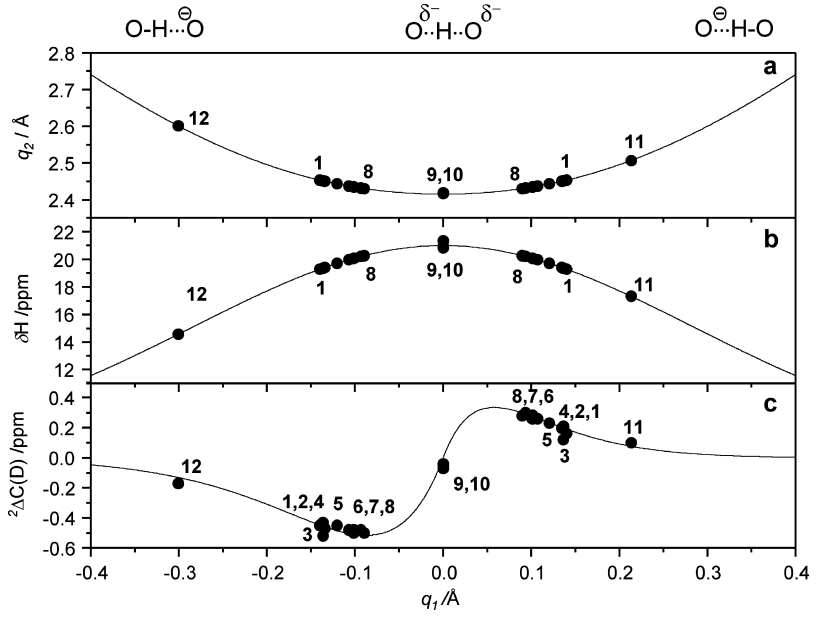

Figure 6. Hydrogen bond correlations for the OHO hydrogen bonds studied in this paper: q_2 (a), δH (b), and $^2\Delta\delta^{13}$C (c) plotted versus q_1. All circles correspond to the intrinsic values of complexes **1**−**12**; see text for more details.

The heteroconjugated anion **11** exhibits a medium-strong hydrogen bond, judging from the proton chemical shift of 17.32 ppm at 120 K. This value is an intrinsic one, i.e. not averaged over two tautomers, as the UV−vis spectrum, measured for the same sample under identical conditions (Figure 4c), only displays a single absorption band around 350 nm. This wavelength is characteristic for complexes where H is located close to the phenolic oxygen, i.e. for a complex of the type $Ph(CH_2)_3COO^-\cdots HOC_6H_4NO_2$.[31] If a second tautomer exhibiting a structure such as $Ph(CH_2)_3COOH\cdots{}^-OC_6H_4NO_2$ would be present, the UV−vis spectrum would contain a second distinct absorption band around 400 nm. Here, from

dx.doi.org/10.1021/jp304943h | J. Phys. Chem. A 2012, 116, 11180−11188

the experimental UV−vis spectrum we estimate that the integrated intensity of such a hidden band will be smaller than 10% of the 350 nm band.[31] The absence of a second minimum on the proton transfer coordinate is schematically depicted in Figure 5c. The positive sign of the H/D isotope effect on the carboxylic carbon chemical shift is indicative of hydrogen bonds where the bridging proton is located on the side of the corresponding carboxylate.[29,30]

The bridging proton of the heteroconjugated anion **12** resonates at 14.6 ppm, at a relatively high field, indicating a significantly longer i.e. weaker hydrogen bond, as compared with complexes **1**−**10**. This finding, combined with the significant difference of the proton accepting abilities of the acetate and of the trifluoroacetate anions (the pK_a values of the corresponding acids in water differ by 4.3 units), allows us to conclude that there is no proton tautomerism and that the observed δH value is intrinsic, corresponding to a $CH_3COOH\cdots{}^{-}OOCCF_3$ structure. This situation is illustrated in Figure 5d. Considering the acetate moiety, the negative sign of the H/D isotope effect on the carboxylic carbon chemical shift is opposite to that of complex **11**. Such negative signs are characteristic for nonionized H-bonded carboxylic groups, in contrast to deprotonated carboxylate anions.[29,30]

Summarizing the results of this subsection, we have established that for **1**−**8** the experimental proton chemical shifts may be affected by a rapid degenerate tautomerism, whereas the spectra of complexes **9**−**12** do not show any indication of such a tautomerism and the observed δH will be intrinsic.

Hydrogen Bond Geometries. In this section we will derive estimates of the hydrogen bond geometries of all the complexes, based on the graphs depicted in Figure 6. We start with eq 3,[22] corresponding to the solid curve in Figure 6b, which provides a link between the proton chemical shifts and the hydrogen bond asymmetry q_1. Thus, we have placed the experimental δH values of all complexes on this curve, obtaining pairs of q_1 values with opposite signs in the case of complexes **1**−**8**, $|q_1|$ and $-|q_1|$, and a single value for complexes **9**−**12**, as illustrated by the circles in Figure 6b. In the next step, we find a set of q_2 values, using the previously published correlation between q_1 and q_2 depicted in Figure 6a.[22] For complexes **9** and **10**, for which a central-symmetric H-bond was found, q_1 was set to 0 and q_2 to its minimum value of 2.415 Å. The resulting hydrogen bond geometries are included in Table 1.

Interestingly, for the homoconjugate anions **1**−**8** the proton displacement upon tautomerisation is quite small, i.e. only between 0.28 and 0.18 Å. This is comparable with the width of the square of the vibrational wave function of the proton[59] and raises the question how well tautomers α and β can be distinguished. Note that the overall hydrogen bond length q_2 and the proton jump distance $q_{1\beta} - q_{1\alpha}$ are monotonously decreasing in the sequence **1**−**8**. This might be an effect of increasingly electronegative substituents in the series: withdrawal of electron density from the oxygen atoms reduces the Coulombic repulsion and allows two carboxylates to approach each other more in the homoconjugated complex. Due to the continuous contraction of the hydrogen bond and the approach of the geometries of two tautomers in the series, eventually the two-point approximation is substituted by a single center-symmetric structure, such as previously reported for hydrogen maleate or $(FHF)^-$ in solution[37] or for other quasi-symmetric structures in solid state listed in ref 39. This means that there is necessarily a region where the distinction of two tautomers looses its physical sense, where an ensemble of interconverting "solvatomers"[53] with slightly different hydrogen bond geometries is realized. To study such an ensemble, NMR spectroscopy should be supplemented by a spectroscopy with a much shorter characteristic time, such as UV−vis.[60] For the purposes of this work, however, the two-state distribution seems to work fine for complexes **1**−**8**.

Correlation between the H/D Isotope Effect on δ^{13}C and Hydrogen Bond Geometry. A correlation of the dependence of the secondary isotope effects $^2\Delta$C(D) on q_1 has been proposed previously on the basis of the valence-bond order model for intermolecular acid−base complexes containing an OHN hydrogen bond.[30] In this work we propose a simple equation which connects explicitly the H/D isotope effect on the carboxylic carbon chemical shift, $^2\Delta$C(D), to the bond asymmetry q_1

$$^2\Delta C(D) = Aq_1\frac{\exp(-B|q_1|)}{1+\exp(Cq_1)} \quad (4)$$

where A, B, and C are fitting parameters. By setting A = 31 ppm·Å^{-1}, B = 13.7 Å^{-1}, and C = 6.1 Å^{-1}, eq 4 becomes in principle equivalent to the equation proposed in ref 30, though it is significantly less cumbersome. The $^2\Delta$C(D) versus q_1 correlation of eq 4 is depicted as a solid line in Figure 6c. The values of H/D isotope effects asymptotically reach zero in the case of the "free" carboxylic acid monomer exhibiting large negative values of q_1 and in the case of the "free" carboxylate anion, characterized by large positive values of q_1. For intermediate values of q_1, the shape of the dependence is dispersion-like. Note that the curve is not fully symmetric with respect to q_1: the span toward the negative values of $\Delta\delta^{13}$C is larger than that toward the positive ones. This is not surprising, because one would expect that the sensitivity of the carboxylic carbon chemical shift to deuteration should eventually decrease when the bridging particle is shifted far from the carboxylate. The asymmetry of the curve is also expected from the experimental data: for complexes **1**−**8** the observed isotope effect is negative, though it is an arithmetic average over two intrinsic values.

The goal of this subsection is to demonstrate that eq 4 with the above-mentioned set of fitting parameters can be applied to the complexes with OHO hydrogen bonds. The data points corresponding to the complexes without proton tautomerism (**9**, **10**, **11**, and **12**) are indeed well located on the curve. By contrast, the data points for the complexes (**1**−**8**) exhibiting a tautomerism are averaged and cannot be placed on the curve directly. To find the intrinsic values of $^2\Delta$C(D) and place them on the curve, one has to take into account that (i) the average of two intrinsic values must equal the experimentally observed isotope effect and that (ii) the intrinsic values of hydrogen bond asymmetry q_1 are given by the experimental values of δH. As shown in Figure 6c, for each complex in the series **1**−**8** under these two restrictions it is possible to find pairs of intrinsic values of $^2\Delta$C(D) in such a way that both values in a pair are lying on the curve in a satisfactory way. The fitted values of intrinsic isotope effects are assembled in Table 1. Summarizing, the whole body of experimental data presented in this work supports the proposed eq 4, and moreover, we show that for homoconjugated complexes eq 4 can be successfully used to extract the intrinsic values of isotope effects from a single experimentally observed averaged value.

It would be very interesting to check the relation between bridging proton position and H/D isotope effect on carboxylic carbon chemical shifts given in eq 4 by quantum-mechanical calculations. Solving the Schroedinger equation to find vibrational wave functions for H and D[61,62] and then convoluting them with shielding surfaces for carbon atoms has previously led to several results, coinciding semiquantitatively with the experiment.[63,28] Making a systematic series of such calculations for a set of homologous complexes along the complete proton transfer pathway in an OHO hydrogen bond remains to be done in the future.

CONCLUSIONS

In this paper, we have studied by NMR inter- and intramolecular hydrogen bonds in a series of homoconjugated anions (**1**−**10** in Figure 1) in polar aprotic solvent. Our main result is a correlation between bridging proton position and the value of H/D isotope effect on carboxylic carbon chemical shift, $^2\Delta C(D)$. This correlation can be used to estimate the hydrogen bond geometry in cases when measurements of bridging proton chemical shift δH are difficult, such as for biomolecules in aqueous solution, where proton exchange hinders the observation of δH.

We would like to conclude our study with the plot shown in Figure 7, which demonstrates one practical aspect of the proposed correlation. The solid line in Figure 7 is based on eqs 3 and 4 and shows the interdependence of two intrinsic NMR parameters: δH and $^2\Delta C(D)$. For the carboxylic acid−carboxylate complexes without proton tautomerism, the observed NMR parameters give data points which lie on the curve (**9**−**12**). In the case of proton tautomerism, the average data point should lie somewhere inside the area contoured by the solid curve (as for **1**−**8**). For example, for homoconjugated anions the average data points should lie on the dotted curve, which is an average of the top and the bottom branches of the solid curve. Besides, for homoconjugates the intrinsic values of $^2\Delta C(D)$ can be found simply as intersections of a vertical line (dashed) with the solid curve (see open circles). In other words, by placing in Figure 7 the data point for an arbitrary carboxylic acid−carboxylate complex, symmetric or otherwise, one should be able to distinguish between the complexes with proton tautomerism (double-well potentials) and without it (single-well potentials).

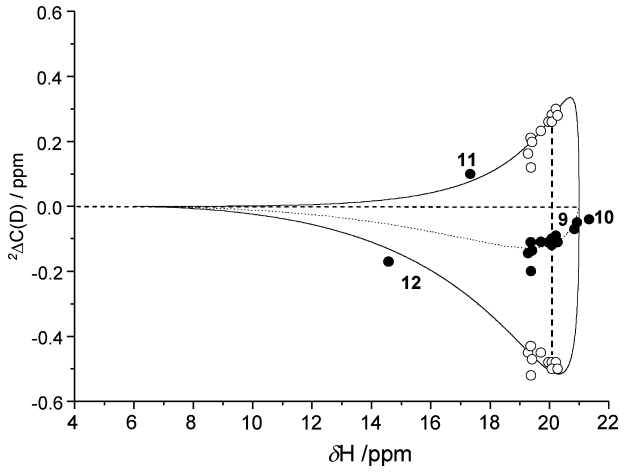

Figure 7. Experimental correlation between proton chemical shift δH and H/D isotope effect on carboxylic carbon chemical shift $^2\Delta\delta^{13}C$. Filled circles are the experimental data points; open circles correspond to the estimated intrinsic values of complexes **1**−**8**. See text for more details.

AUTHOR INFORMATION

Notes

The authors declare no competing financial interest.

ACKNOWLEDGMENTS

We thank Dr. E. T. J. Nibbering, Max-Born Institute, Berlin, for helpful discussions. This work has received financial support from the Deutsche Forschungsgemeinschaft, Bonn, the Russian Foundation of Basic Research, and the European Research Council under the European Union's Seventh framework Program (FP7/2007-2013/ERC grant agreement No. 247051 T.E.).

REFERENCES

(1) (a) Katz, B. A.; Erlod, K.; Luong, C.; Rice, M. J.; Mackman, R. L.; Sprengeler, P. A.; Spencer, J.; Hataye, J.; Janc, J.; Link, J.; et al. *J. Mol. Biol.* **2001**, *307*, 1451−1486. (b) Northrop, D. B. *Acc. Chem. Res.* **2001**, *34*, 790−797. (c) Kim, K. S. *Biochemistry* **2002**, *41*, 5300−5306.

(2) Smith, R.; Brereton, I. M.; Chai, R. Y.; Kent, S. B. H. *Nat. Struct. Biol.* **1996**, *3*, 946−950.

(3) Anderson, S.; Crosson, S.; Moffat, K. *Acta Crystallogr.* **2004**, *D60*, 1008−1016.

(4) Cleland, W. W.; Kreevoy, M. M. *Science* **1994**, *264*, 1887−1890.

(5) Tobin, J. B.; Whitt, S. A.; Cassidy, C. S.; Frey, P. A. *Biochemistry* **1995**, *34*, 6919−6924.

(6) Wallace Cleland, W.; Frey, P. A.; Gerlt, J. A. *J. Biol. Chem.* **1998**, *273*, 25529−25532.

(7) Gilli, P.; Bertolasi, V.; Pretto, L.; Ferretti, V.; Gilli, G. *J. Am. Chem. Soc.* **2004**, *126*, 3845−3855.

(8) Langkilde, A.; Kristensen, S. M.; Lo Leggio, L.; Moelgaard, A.; Jensen, J. H.; Houk, A. R.; Navarro Poulsen, J.-C.; Kauppinen, S.; Larsen, S. *Acta Crystallogr. D* **2008**, *D64*, 851−863.

(9) Piana, S.; Bucher, D.; Carloni, P.; Rothlisberger, U. *J. Phys. Chem. B* **2004**, *108*, 11139−11149.

(10) Steiner, T.; Saenger, W. *J. Am. Chem. Soc.* **1992**, *114*, 7123−7126.

(11) Steiner, T.; Saenger, W. *Acta Crystallogr. B* **1994**, *B50*, 348−357.

(12) Steiner, T. *J. Chem. Soc., Chem. Commun.* **1995**, 1331−1332.

(13) Limbach, H. H.; Pietrzak, M.; Benedict, H.; Tolstoy, P. M.; Golubev, N. S.; Denisov, G. S. *J. Mol. Struct.* **2004**, *706*, 115−119.

(14) Limbach, H. H.; Pietrzak, M.; Sharif, S.; Tolstoy, P. M.; Shenderovich, I. G.; Smirnov, S. N.; Golubev, N. S.; Denisov, G. S. *Chem.—Eur. J.* **2004**, *10*, 5195−5204.

(15) Sharif, S.; Denisov, G. S.; Toney, M. D.; Limbach, H. H. *J. Am. Chem. Soc.* **2007**, *129*, 6313−6327.

(16) Sharif, S.; Schagen, D.; Toney, M. D.; Limbach, H. H. *J. Am. Chem. Soc.* **2007**, *129*, 4440−4455.

(17) Sharif, S.; Fogle, E.; Toney, M. D.; Denisov, G. S.; Shenderovich, I. G.; Buntkowsky, G.; Tolstoy, P. M.; Chan Huot, M.; Limbach, H. H. *J. Am. Chem. Soc.* **2007**, *129*, 9558−9559.

(18) Limbach, H. H.; Chan-Huot, M.; Sharif, S.; Tolstoy, P. M.; Shenderovich, I. G.; Denisov, G. S.; Toney, M. D. *Biochim. Biophys. Acta, Proteins Proteomics* **2011**, *1814*, 1426−1437.

(19) Sternberg, U.; Brunner, E. L. *J. Magn. Reson. A* **1994**, *108*, 142−150.

(20) Sigala, P. A.; Tsuchida, M. A.; Herschlag, D. *Proc. Natl. Acad. Sci.* **2009**, *106*, 9232−9237.

(21) (a) Libowitzki, E. *Monatsh. Chem.* **1999**, *130*, 1047−1059. (b) Emsley, J. *Chem. Soc. Rev.* **1980**, *9*, 91−124. (c) Mikenda, W. *J. Mol. Struct.* **1986**, *147*, 1−15. (d) Novak, A. *Struct. Bonding (Berlin)* **1974**, *18*, 177−216.

(22) Limbach, H. H.; Tolstoy, P. M.; Pérez-Hernández, N.; Guo, J.; Shenderovich, I. G.; Denisov, G. S. *Isr. J. Chem.* **2009**, *49*, 199−216.
(23) Detering, C.; Tolstoy, P. M.; Golubev, N. S.; Denisov, G. S.; Limbach, H.-H. *Dokl. Phys. Chem.* **2001**, *379*, 1−4.
(24) (a) Chen, J.-H.; Mao, X.-A. *J. Magn. Reson.* **1998**, *131*, 358−361. (b) Grzesiek, S.; Bax, A. *J. Am. Chem. Soc.* **1993**, *115*, 12593−12594.
(25) Gu, Z.; McDermott, A. *J. Am. Chem. Soc.* **1993**, *115*, 4282−4285.
(26) Gu, Z.; Zambrano, R.; McDermott, A. *J. Am. Chem. Soc.* **1994**, *116*, 6368−6372.
(27) Facelli, J. C.; Gu, Z.; McDermott, A. *Mol. Phys.* **1995**, *86*, 865.
(28) Piana, S.; Sebastiani, D.; Carloni, P.; Parrinello, M. *J. Am. Chem. Soc.* **2001**, *123*, 8730−8737.
(29) Tolstoy, P. M.; Schah-Mohammedi, P.; Smirnov, S. N.; Golubev, N. S.; Denisov, G. S.; Limbach, H. H. *J. Am. Chem. Soc.* **2004**, *126*, 5621−5634.
(30) Tolstoy, P. M.; Guo, J.; Koeppe, B.; Golubev, N. S.; Denisov, G. S.; Smirnov, S. N.; Limbach, H.-H. *J. Phys. Chem. A* **2010**, *114*, 10775−10782.
(31) Koeppe, B.; Tolstoy, P. M.; Limbach, H. H. *J. Am. Chem. Soc.* **2011**, *133*, 7897−7908.
(32) (a) Pan, Y.; McAllister, M. A. *J. Am. Chem. Soc.* **1997**, *119*, 7561−7566. (b) Basch, H.; Stevens, W. J. *J. Am. Chem. Soc.* **1991**, *113*, 95−101.
(33) Limbach, H. H.; Schowen, K. B.; Schowen., R. L. *J. Phys. Org. Chem.* **2010**, *23*, 586−605.
(34) Limbach, H. H.; Lopez, J. M.; Kohen, A. *Philos. Trans. B (London)* **2006**, *361*, 1399−1415.
(35) (a) Horsewill, A. J.; Jones, N. H.; Caciuffo, R. *Science* **2001**, *291*, 100−103. (b) Waluk, J. *Isr. J. Chem.* **2009**, *49*, 175−185. (c) Reynhardt, E. C.; Latanowicz, L. *J. Magn. Reson.* **1998**, *130*, 195−208.
(36) Guo, J.; Tolstoy, P. M.; Koeppe, B.; Denisov, G. S.; Limbach, H.-H. *J. Phys. Chem. A* **2011**, *115*, 9828−9836.
(37) Schah-Mohammedi, P.; Shenderovich, I. G.; Detering, C.; Limbach, H.-H.; Tolstoy, P. M.; Smirnov, S. N.; Denisov, G. S.; Golubev, N. S. *J. Am. Chem. Soc.* **2000**, *122*, 12878−12879.
(38) Siegel, J. S.; Anet, F. A. I. *J. Org. Chem.* **1988**, *53*, 2629−2630.
(39) (a) Steiner, T. *J. Phys. Chem. A* **1998**, *102*, 7041−7052. (b) Steiner, T.; Wilson, C. C.; Majerz, I. *Chem. Commun.* **2000**, 1231−1232.
(40) Pauling, L. *J. Am. Chem. Soc.* **1947**, *69*, 542−553.
(41) Brown, I. D. *Acta Crystallogr.* **1992**, *B48*, 553−572.
(42) Emmler, T.; Gieschler, S.; Limbach, H. H.; Buntkowsky, G. *J. Mol. Struct.* **2004**, *700*, 29−38.
(43) Lorente, P.; Shenderovich, I. G.; Golubev, N. S.; Denisov, G. S.; Buntkowsky, G.; Limbach, H. H. *Magn. Reson. Chem.* **2001**, *39*, S18−S29.
(44) Shenderovich, I. G.; Limbach, H. H.; Smirnov, S. N.; Tolstoy, P. M.; Denisov, G. S.; Golubev, N. S. *Phys. Chem. Chem. Phys.* **2002**, *4*, 5488−5497.
(45) Shenderovich, I. G.; Tolstoy, P. M.; Golubev, N. S.; Smirnov, S. N.; Denisov, G. S.; Limbach, H. H. *J. Am. Chem. Soc.* **2003**, *125*, 11710−11720.
(46) Smirnov, S. N.; Benedict, H.; Golubev, N. S.; Denisov, G. S.; Kreevoy, M. M.; Schowen, R. L.; Limbach, H. H. *Can. J. Chem.* **1999**, *77*, 943−949.
(47) (a) Kymtis, L.; Mikulskis, P. *J. Magn. Reson.* **1975**, *20*, 475. (b) Lumbroso-Bader, N.; Coupry, C.; Baron, D.; Govil, G. *J. Magn. Reson.* **1975**, *17*, 386−392.
(48) Golubev, N. S. *Khim. Fiz.* **1984**, *3*, 772−774.
(49) Golubev, N. S.; Melikova, S. M.; Shchepkin, D. N.; Shenderovich, I. G.; Tolstoy, P. M.; Denisov, G. S. *Z. Phys. Chem.* **2003**, *217*, 1549−1563.
(50) Perrin, C. L.; Nielson, J. B. *J. Am. Chem. Soc.* **1997**, *119*, 12734−12741.
(51) Guo, J.; Koeppe, B.; Tolstoy, P. M. *Phys. Chem. Chem. Phys.* **2011**, *13*, 2335−2341.
(52) Garcia-Viloca, M.; Gonzalez-Lafont, A.; Lluch, J. M. *J. Am. Chem. Soc.* **1999**, *121*, 9198−9207.
(53) Perrin, C. L.; Lau, J. S. *J. Am. Chem. Soc.* **2006**, *128*, 11820−11824.
(54) Golubev, N. S.; Denisov, G. S.; Smirnov, S. N.; Shchepkin, D. N.; Limbach, H. H. *Z. Phys. Chem.* **1996**, *196*, 73−84.
(55) (a) Gunnarsson, G.; Wennerstrom, H.; Egan, W.; Forsen, S. *Chem. Phys. Lett.* **1976**, *38*, 86−99. (b) Altman, L. J.; Laungani, D.; Gunnarsson, G.; Wennerstrom, H.; Forsen, S. *J. Am. Chem. Soc.* **1978**, *100*, 8264−8266.
(56) Kueppers, H.; Takusagawa, F.; Koetzle, T. F. *J. Chem. Phys.* **1985**, *82*, 5636−5647.
(57) Perrin, C. L. *Acc. Chem. Res.* **2010**, *43*, 1550−1557.
(58) Bogle, X. S.; Singleton, D. A. *J. Am. Chem. Soc.* **2011**, *133*, 17172−17175.
(59) Steiner, T.; Majerz, I.; Wilson, C. C. *Angew. Chem., Int. Ed.* **2001**, *40*, 2651−2656.
(60) Tolstoy, P. M.; Koeppe, B.; Denisov, G. S.; Limbach, H. H. *Angew. Chem., Int. Ed.* **2009**, *48*, 5745−5747.
(61) Pirc, G.; Mavri, J.; Stare, J. *Vib. Spectrosc.* **2012**, *58*, 153−162.
(62) Schmidt, B.; Lorenz, U. *WavePacket 4.8: A program package for quantum-mechanical wavepacket propagation and time-dependent spectroscopy*. Available via http://wavepacket.sourceforge.net (2011).
(63) Stare, J.; Jezierska, A.; Ambrožic, G.; Košir, I. J.; Kidrič, J.; Koll, A.; Mavri, J.; Hadzi, D. *J. Am. Chem. Soc.* **2004**, *126*, 4437−4443.